

CD1a-Expressing Monocytes as Mediators of Inflammation in Ulcerative Colitis

Omar Al-amodi,* Henrika Jodeleit, DVM,[†] Florian Beigel, MD,[‡] Eckhard Wolf, DVM,[†] Matthias Siebeck, MD,* and Roswitha Gropp, PhD*

Background: CD1a-expressing CD14⁺ monocytes have been identified as inducers of autoreactive T cells. In this study, the link between inflammatory and metabolic signals and CD1a-expressing monocytes in vitro and in vivo was examined, and CD1a was evaluated as a potential therapeutic target for treatment of ulcerative colitis (UC).

Methods: Peripheral blood mononuclear cells (PBMCs) from UC patients and non-UC donors were incubated with phosphatidylcholine (PC) for 2 and 7 days and subjected to flow cytometric analysis. Triacylglycerol (TAG) and cholesterol levels and frequencies of CD14⁺ CD1a⁺ monocytes were determined in a mouse model of UC that is based on NOD/scid IL2R γ^{null} mice reconstituted with PBMCs from UC patients (NSG-UC). NSG-UC mice were treated with anti-CD1a antibodies. Response to treatment was determined by clinical and histological scores, flow cytometric analysis of human leucocytes from the spleen and colon, and expression levels of TGF β 1, HGF, IFN γ , and TARC.

Results: Incubation of PBMCs with PC resulted in an increase of the frequency of CD1a⁺ CD14⁺ monocytes at the expense of CCR2⁻, CD86⁻, and TSLPR-expressing CD14⁺ monocytes. CD1a⁺ CD14⁺ monocytes induced the activation of CD4⁺ T cells and differentiation of Th cells. In vivo, TAG and cholesterol levels increased upon inflammation and correlated positively with CD14⁺ CD1a⁺ monocytes. NSG-UC mice benefitted from treatment with anti-CD1a antibodies, as indicated by a reduced histological score and reduced frequencies of CD1a⁺ CD14⁺ monocytes in the colon and spleen of mice.

Conclusion: CD1a-expressing monocytes might act as sensors and mediators of inflammation in UC. Mice benefitted from treatment with anti-CD1a antibodies.

Key Words: ulcerative colitis, CD1a, macrophage, monocyte, metabolic, inflammation

INTRODUCTION

CD1a has long been known as a marker of Langerhans cells. Langerhans cells originate from yolk sac–derived erythro-myeloid progenitors, populate the epidermis during embryonic development, and maintain themselves during adulthood independent of hematopoiesis.^{1,2} In contrast, embryonic macrophages of the intestine are replaced by monocyte-derived

macrophages after birth and are constantly replenished by recruited monocytes during adulthood.³ Recently, CD1a expression has also been found in monocyte-derived dendritic cells (moDCs) of the intestine.⁴ One hallmark of these cells is the expression of IL-12.⁵ CD1a belongs to the CD1 family of antigen-presenting proteins, which activate T cells by presenting lipids. It has long been considered an alternative system to complement the defense against pathogens that is mainly driven by peptide antigen-presenting major histocompatibility complex. In the meantime, however, it has been found that CD1a and b also present self-lipids such as phosphatidylcholine (PC) or triacylglycerol (TAG) to induce autoreactive T cells.^{6–9} Unlike the CD1d restricted natural killer T cells, T cells recognizing CD1a belong to the normal $\alpha\beta$ T-cell repertoire and present a population of 0.02%–0.4% in healthy individuals.⁸ T cells that reacted to presentation via CD1a with the release of IL-13, IFN γ , and IL-22 and were identified as Th22 cells. This analysis was performed with healthy donors, and as T cells expressed CLA, it has been suggested that auto-reactivity is a normal response in the skin provoked by injury to induce the wound healing processes. We have recently identified CD1a-expressing CD11b⁺ macrophages and CD14⁺ monocytes as biological markers to discriminate between patients with ulcerative colitis (UC) and non-UC donors with high sensitivity and specificity.¹⁰ In addition, both cellular populations were found to be elevated in colon specimens of UC

Received for publications June 9, 2017; Editorial Decision January 5, 2018.

From the *Department of General-Visceral-, Vascular- and Transplantation Surgery, Hospital of the LMU, Munich, Germany; [†]Institute of Molecular Animal Breeding and Biotechnology, and Laboratory for Functional Genome Analysis (LAFUGA), Gene Center, LMU Munich, Munich, Germany; [‡]Department of Medicine II-Grosshadern, Hospital of the LMU Munich, München, Germany

Conflicts of interest: The authors have no conflicts of interest to declare.

Supported by: This work was funded by the Bundesministerium für Bildung und Forschung (grant No. 03V0556, 03V0558).

Address correspondence to: Roswitha Gropp, PhD, Department of General-, Visceral-, and Transplantation Surgery, Hospital of the LMU, Nussbaumstraße 20, 80336 Munich, Germany (roswitha.gropp@med.uni-muenchen.de).

© 2018 Crohn's & Colitis Foundation. Published by Oxford University Press on behalf of Crohn's & Colitis Foundation.

This is an Open Access article distributed under the terms of the Creative Commons Attribution Non-Commercial License (<http://creativecommons.org/licenses/by-nc/4.0/>), which permits non-commercial re-use, distribution, and reproduction in any medium, provided the original work is properly cited. For commercial re-use, please contact journals.permissions@oup.com

doi: 10.1093/ibd/izy073

Published online 17 May 2018

patients as compared with non-UC specimens. Furthermore, both cell types were identified as inflammatory markers in the NSG-UC mouse model,¹¹ suggesting that CD1a monocytes and macrophages elicit a proinflammatory immune response. In the inflammatory setting, the supply of fatty acid ligands could be provided by PLA2—an important component of inflammation and bee and wasp venom.¹² PLA2 releases fatty acids from phospholipids and thus could enhance inflammation via CD1a. This hypothesis is corroborated by the finding that PLA2 levels were increased in the NSG-UC mouse model (our own results). Alternatively, the metabolic switch observed in response to inflammation might provide lipids.

In this study, we examined the role of CD1a-expressing monocytes and macrophages in UC *in vitro* and *in vivo*. We first examined the effect of PC on monocytes and macrophages *in vitro*. Incubation of peripheral blood mononuclear cells (PBMCs) with PC resulted in increased frequencies of CD14+ CD1a+ monocytes at the expense of TSLPR-expressing monocytes and diminished frequencies of Tregs, suggesting a pathological phenotype of CD1a-expressing monocytes. In addition, PC induced the activation of CD4+ T cells via CD1a. This expression pattern of CD1a-expressing monocytes was corroborated by *ex vivo* analysis. In UC patients, co-expression of TSLPR was decreased as compared with nondiseased individuals. Furthermore, we analyzed the correlation of TAG- and cholesterol levels with frequencies of CD14+ CD1a+ monocytes in the NSG-UC mouse model. Both lipids correlated positively with CD14+ CD1a+ monocytes. Finally, NSG-UC mice were treated with an anti-CD1a antibody to corroborate the hypothesis that CD1a+ monocytes elicit a proinflammatory response. Mice benefited from treatment, as indicated by a diminished histological score. In addition, treatment with anti-CD1a antibodies specifically affected frequencies of CD14+ CD1a+ monocytes in the colon and the spleen and resulted in increased mRNA expression levels of TGF β 1 and TARC in distal parts of the colon. In contrast, HGF mRNA levels decreased, suggesting that treatment with anti-CD1a antibodies suppresses acute inflammation and favors the remodeling of the colon.

METHODS

Isolation of PBMCs and Engraftment

Sixty milliliters of peripheral blood was collected from the arm vein of patients suffering from UC in trisodium citrate solution (S-Monovette, Sarstedt, Nürnberg, Germany). The blood was diluted with Hank's balanced salt solution (HBSS; Sigma Aldrich, Deisenhofen, Germany) in a 1:2 ratio, and 30 mL of the suspension was loaded onto LeucoSep tubes (Greiner Bio One, Frickenhausen, Germany). PBMCs were separated by centrifugation at 400g for 30 minutes with no deceleration. The interphase was extracted and diluted with phosphate buffered saline (PBS) to a final volume of 40 mL. Cells were counted and centrifuged at 1400 g for 5 minutes.

The cell pellet was resuspended in PBS at a concentration of 4×10^6 cells in 100 μ L.

Six- to 8-week-old NSG mice were engrafted with 100- μ L cell suspension into the tail vein on day 1.

Cell Culture

PBMCs of UC patients and healthy individuals were isolated. The cell pellet was resuspended in RPMI (Thermo Fisher Scientific, Waltham, MA, USA) at a concentration of 1×10^6 cells/mL. Additionally, 500- μ L RPMI with 10% FCS and 1% penicillin-streptomycin (Sigma-Aldrich, St. Louis, MO, USA) were added to each well and sample. Wells containing PBMCs and RPMI or PBMCs, RPMI and 10 μ g of phytohemagglutinin (PHA)/mL served as negative and positive controls, respectively. For analysis of the effect of PC on PBMCs, 200 μ g/mL PC (Sigma-Aldrich, St. Louis, MO, USA) was added. Cells were incubated for 48 hours and labeled for flow cytometry.

To analyze the effect of an anti-CD1a antibody on cells stimulated with PC, cells were incubated for 1 hour with 10 μ g/mL of anti-human CD1a (Bio X Cell, West Lebanon, USA) and 10 μ g/mL of a corresponding isotype antibody (Biolegend, San Diego, CA, USA) before 200 μ g/mL of PC (Sigma-Aldrich, St. Louis, USA) was added. All wells additionally contained 15 ng/mL of IL-2 and IL-15 (PeproTech GmbH, Hamburg, Deutschland). Cells were incubated for 2 or 7 days and then labeled for flow cytometry.

To examine proliferation of CD14+ CD1a+ monocytes, cells were stained with the CellTrace CFSE Cell Proliferation Kit (Thermo Fisher Scientific, Waltham, MA, USA) according to the manufacturer's instructions. Cells were incubated for 5 days before flow cytometry analysis was performed.

Animal Study Protocol

NOD/scid IL-2R γ^{null} mice were obtained from Charles River Laboratories (Sulzfeld, Germany). Mice were kept under specific pathogen-free conditions in individually ventilated cages in a facility controlled according to the Federation of Laboratory Animal Science Association guidelines. Following engraftment (day 1), mice were presensitized by rectal application of 150 μ L of 10% ethanol on day 8 using a 1-mm cat catheter (Henry Schein, Hamburg, Germany). The catheter was lubricated with Xylocain Gel 2% (AstraZeneca, Wedel). Rectal application was performed under general anaesthesia using 4% Isofluran. Postapplication, mice were kept at an angle of 30° to avoid ethanol dripping. On days 15 and 18, mice were challenged by rectal application of 50% ethanol following the protocol of day 8. Mice were killed on day 21.

Mice were treated by intraperitoneal application of 30 μ g of anti-CD1a antibody (Clone OKT6, BioXcell, West Lebanon, USA) or 30 μ g of isotype control (Biolegend, San Diego, CA, USA) on days 7, 14, and 17.

Clinical Activity Score

The assessment of colitis severity was performed daily according to the following scoring system: Loss of body weight: 0% (0), 0%–5% (1), 5%–10% (2), 10%–15% (3), 15%–20% (4). Stool consistency: formed pellet (0), loose stool or unformed pellet (2), liquid stools (4). Behavior: normal (0), reduced activity (1), apathy (4), and ruffled fur (1). Body posture: intermediately hunched posture (1), permanently hunched posture (4). The scores were added daily for a total score with a maximum of 18 points per day. Animals who suffered from weight loss >20%, rectal bleeding, rectal prolapse, self-isolation, or a severity score >7 were killed immediately and not taken into count.

Histological Analysis

Samples from distal parts of the colon were fixed in 4% formaldehyde for 24 hours, before storage in 70% ethanol, and were routinely embedded in paraffin. Samples were cut into 3- μ m sections and stained with hematoxylin and eosin (H&E). Epithelial erosions were scored as follows: no lesions (0), focal lesions (1), multifocal lesions (2), major damage with involvement of basal membrane (3). Inflammation was scored as follows: infiltration of few inflammatory cells into the lamina propria (1), major infiltration of inflammatory cells into the lamina propria (2), confluent infiltration of inflammatory cells into the lamina propria (3), infiltration of inflammatory cells including tunica muscularis (4). Fibrosis was scored as follows: focal fibrosis (1), multifocal fibrosis and crypt atrophy (2). The presence of edema, hyperemia, and crypt abscess was scored with 1 additional point in each case. The scores for each criterion were added for a total score ranging from 0 to 12. Images were taken with a Zeiss AxioVert 40 CFL camera. Figures show representative longitudinal sections in original magnification. In Adobe Photoshop CS6, a tonal correction was applied in order to enhance contrasts within the pictures.

Isolation of Human Leucocytes

To isolate human leucocytes from murine spleen, spleens were minced and cells filtrated through a 70- μ L cell strainer (Greiner Bio-One, Frickenhausen), followed by centrifugation at 1400 g for 5 minutes, and resuspended in FACS buffer (1 \times PBS, 2 mM EDTA, 2% FCS). For further purification, cell suspensions were filtrated using a 35- μ m cell strainer (Greiner Bio-One, Frickenhausen) and then labeled for flow cytometry analysis.

Flow Cytometry Analysis

Labeling of human leucocytes was performed according to [Supplementary Table 2](#). All antibodies were purchased from Biolegend (San Diego, CA, USA), with the exception of the intracellular staining of the Th subsets, which were purchased from R&D Systems (Heidelberg, Germany). All antibodies were used according to the manufacturer's instructions. Flow

cytometry was performed using a BD FACS Canto II and analyzed with FlowJo 10.1-Software (FlowJo LLC, OR, USA). Cells were quantified according to the gating strategy depicted in [Supplementary Figure 1](#).

RNA Analysis

RNA extraction and cDNA synthesis

Approximately 1 cm of distal parts of the colon was disrupted and homogenized with a TissueLyser LT (Qiagen, Hilden, Germany) followed by total RNA extraction according to the manufacturer's instruction using RNeasy Plus Universal Mini Kit (Qiagen, Hilden, Germany) and chloroform (Sigma-Aldrich, St. Louis, MO, USA). No further treatment with DNase was needed as gDNA Eliminator Solution was included in the kit.

Reverse Transcription of RNA

Five μ g of total RNA were used for cDNA synthesis. Reverse transcription was performed using a Mastercycler gradient (Eppendorf, Hamburg, Germany) and QuantiNova Reverse Transcription Kit (Qiagen, Hilden, Germany). To obtain a cDNA concentration between 10 pg and 100 ng, as required by the TaqMan Fast Advanced Master Mix protocol (Thermo Fisher Scientific, Waltham, MA, USA), samples were diluted with RNase-free water.

RNA and cDNA purity was assessed using a Nanodrop 2000 spectrophotometer (Thermo Fisher Scientific, Waltham, MA, USA).

Quantitative Real-time Polymerase Chain Reaction

Quantitative real-time polymerase chain reaction (RT-PCR) was performed according to the TaqMan Fast Advanced Master Mix protocol (Thermo Fisher Scientific, Waltham, MA, USA) using the Applied Biosystems StepOnePlus real-time PCR system (Thermo Fisher Scientific, Waltham, MA, USA). Single Tube TaqMan Gene Expression Assays (Thermo Fisher Scientific, Waltham, MA, USA) included primers for the housekeeping genes GAPDH (Mm99999915_g1), GUSB (Mm00446953_m1), and TGF β (Mm01178820_m1), HGF (Hs04329698_m1), CCL17 (Mm01244826_g1), and IFN γ (Hs00989291_m1). Analysis was performed using StepOnePlus Software v2.3.

The mean cycle threshold (CT) value was calculated for the housekeeping genes. Relative expression values for the analyzed genes were calculated as the difference between the mean cycle threshold (CT) of the housekeeping genes and the analyzed gene (delta CT) and depicted as the logarithmic value.

Detection of Cholesterol and Triglycerol Levels

Cholesterol and triglycerol levels were determined enzymatically by the Institute of Laboratory Medicine LMU,

Munich, Germany, using the Cobas analyzer (Roche Diagnostics, Mannheim, Germany).

Statistics

Statistical analysis was performed with R: A language and environment for statistical computing (R Foundation for Statistical Computing, Vienna, Austria; <https://www.R-project.org/>) and BRB Array Tools (<https://brb.nci.nih.gov/BRB-ArrayTools/>). Variables were represented with mean, standard deviation, median, and interquartile range values. A 2-sided Student *t* test and a confidence level of 0.95 were used to compare binary groups, and for more than 2 groups, analysis of variance (ANOVA), followed by TukeyHSD, was conducted. For correlation analysis, Spearman or Pearson correlation was used.

RESULTS

Phosphatidylcholine Affects Differentiation of CD14+ Monocytes and Regulatory T Cells

PC and derivatives of PC are important mediators of inflammation and resolution of inflammation. As PC has been described as a natural ligand of CD1a,⁷ we examined the effect of PC on monocytes and macrophages; 1×10^6 / mL PBMCs derived from UC patients ($n = 13$) and non-UC donors ($n = 28$) was incubated in the presence (PC $n = 41$) or absence (control $n = 39$) of PC, as described in the Methods section. PHA served as a control antigen ($n = 40$). As shown in **Figure 1A**, frequencies of CD14+ CD1a+ monocytes increased significantly in the presence of PC, whereas PHA had no effect (for the complete data set, see **Supplementary Table 3**). In contrast, frequencies of CD14+ CD86+ declined upon incubation with PC, and CD14+ TSLPR+ declined in the presence of PC and PHA. PC had no effect on CD11b+ CD1a+ macrophages. In contrast to PHA, incubation with PC resulted in a significant decrease of regulatory T cells (Treg), indicating that PC elicits a proinflammatory response. As CD1a is thought to activate autoreactive T cells that are a considered a normal component of the human $\alpha\beta$ T cell repertoire, a correlation analysis was performed between frequencies of CD14+ CD1a+ monocytes and Th1 and Th2 cells (**Fig. 1B**). Frequencies of Th1 and Th2 cells correlated positively with frequencies of CD1a+ CD14+, and both correlations were significant, further corroborating the linkage between CD1a+ monocytes and T cells.

In order to examine whether PC induced the proliferation of CD1a-expressing monocytes, cell trace dilution was examined as described in the Methods section (**Fig. 1C**). Prior to incubation, PBMCs were stained with CellTrace CFSE. As shown in **Figure 1C**, PC induced the proliferation of CD14+ CD1a monocytes.

By using tetramers, previous studies have identified a natural subset of CD4+ as target cells of CD1a.⁸ To corroborate

these results and the correlation analysis, PBMCs from 4 different donors were incubated with PC, and CD4+ T cells were analyzed for intracellular expression of IFN γ , IL-4, and IL-17. We observed an increase of all 3 populations, and this increase was significant for CD4+ IFN γ +. This effect could partially be reversed by anti-CD1a antibody.

To further examine whether CD1a mediates responses to CD4+ T cells, PBMCs from 2 different donors were incubated for 7 days with PC in the presence of absence of anti-CD1a antibodies adapted to the protocol described in de Jong et al. [8]. PHA served as a positive control (for the complete data set, see **Supplementary Table 3**). As observed after incubation for 2 days, frequencies of CD1a-expressing monocytes were significantly increased in the presence of PC (**Fig. 2**). Anti-CD1a antibodies had no effect. This also applies to regulatory T cells (CD4+ CD25+ CD127 low), indicating that this effect was not mediated by CD1a. The effect of PC on activated CD4+ T cells (CD4+ CD69+ and CD4+ CD134+) and mucosal CD4+ T cells (CD4+ CD103+), however, seemed to be mediated by CD1a as frequencies of these cell types increased and the effect was abolished in the presence of anti-CD1a antibodies. In contrast to previous results, which described an induction of Th22 cells by CD1a,⁷ a decline of Th22 was observed.

CD14+ CD1a+ Monocytes Display a Proinflammatory Phenotype Ex Vivo

As in vitro data might not reflect the in vivo situation, the CD14+ CD1a+ monocyte population was further analyzed for expression of CCR2, CD86, TSLPR, and CD1a in PBMCs from UC ($n = 21$) and non-UC donors ($n = 9$). As shown in **Figure 3**, there was a significant difference in the CD14+ CD1a+ coexpression pattern between non-UC and UC patients. The CD14+ CD1a+ population from UC patients displayed a higher activation status, higher CCR2 levels to direct them to sites of inflammation, and lower levels of TSLPR. The latter observation is in agreement with the results obtained in vitro and supports the assumption that CD1a+ monocytes shift the balance toward a proinflammatory phenotype in UC. Assuming that the coexpression pattern of the non-UC patient reflects the normal situation, CD14+ CD1a+ monocytes are furnished to convey signals toward a proinflammatory or immune-tolerating and remodeling response depending on the level of expression of receptors on CD14+ CD1a monocytes and factors released from the inflammatory milieu signals.

TAG and Cholesterol Levels Correlate With CD14+ CD1a+ Monocytes In Vivo

The strong response to exposure with PC suggested that CD1a+ CD14+ monocytes might respond to inflammation by proliferation and differentiation. As TAG and/or cholesterol have been found elevated in chronic diseases¹³ and have

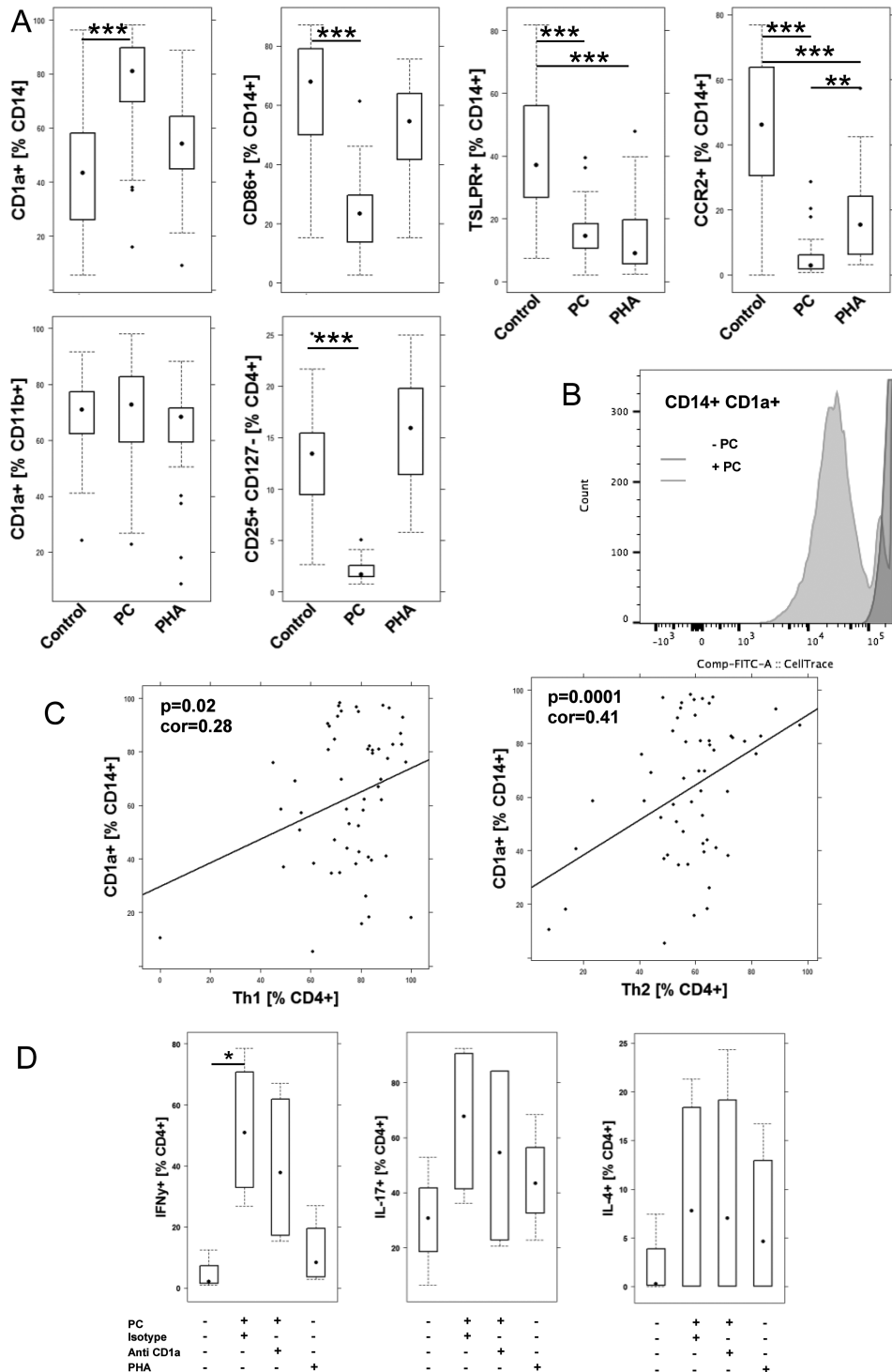


FIGURE 1. Incubation of PBMCs with PC affects frequencies of monocytes, macrophages, and CD4 T cells. A, Flow cytometric analysis of PBMCs from UC patients (n = 13) and non-UC donors (n = 28) that were incubated in the absence of PC (control n = 39) or presence of PC (n = 41) and PHA (n = 40) for 48 hours depicted as boxplot diagrams. B, Cell trace CFSE dilution of CD14+ CD1a+ monocytes. C, Correlation analysis of frequencies of CD14+ CD1a+ monocytes and Th1 of Th2 cells depicted as scatter plots. The method was Pearson; numbers display correlation coefficients (cor-values) and P values. D, Flow cytometric analysis of CD4+ T cells for intracellular expression of IFN γ , IL-4, or IL-17 depicted as boxplots. PBMCs (n = 4) were incubated in the absence or presence of PC and anti-CD1a antibody. For comparison of groups, ANOVA followed by Tukey's HSD was conducted. Boxes represent upper and lower quartiles, whiskers represent variability, and outliers are plotted as individual points (** <0.001 ; * <0.01 ; * <0.05).

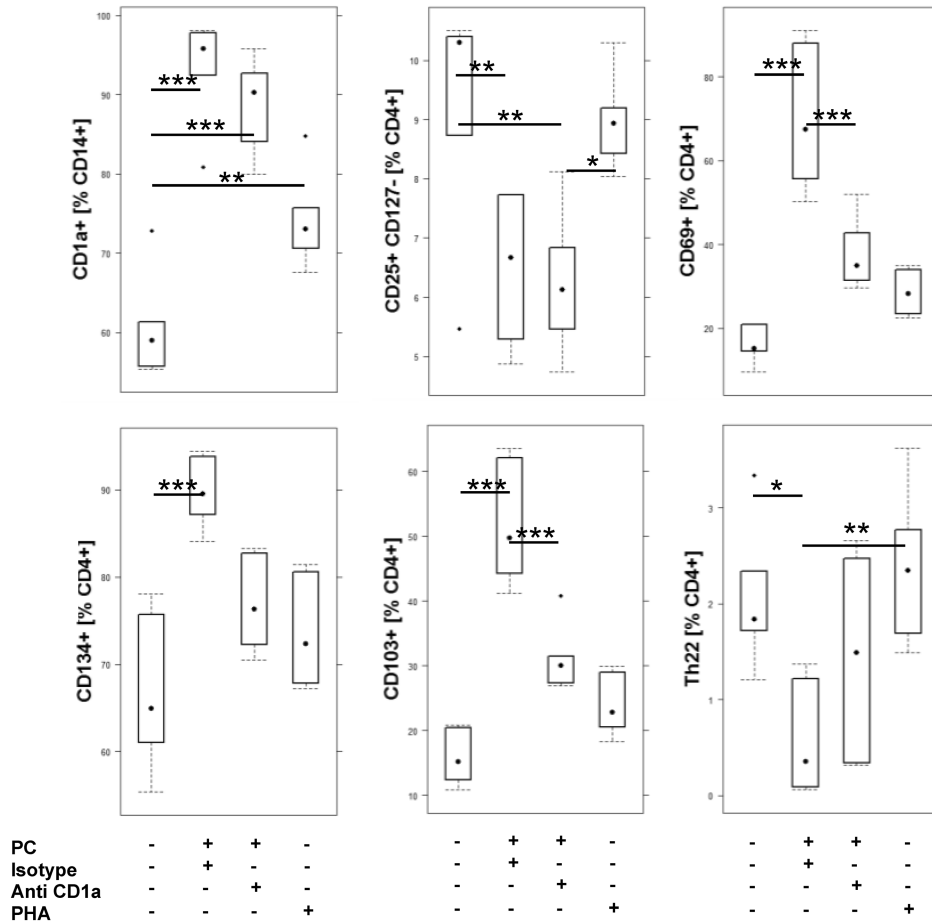


FIGURE 2. Anti-CD1a antibodies affect frequencies of CD4+ T cells. Flow cytometric analysis of PBMCs from 2 different donors that were incubated in triplicate for 5 days with PC in the presence (n = 6) or absence of anti-CD1a antibodies (n = 6) or PHA (n = 6) depicted as boxplot diagrams. For comparison of groups, ANOVA followed by Tukey’s HSD was conducted. Boxes represent upper and lower quartiles, whiskers represent variability, and outliers are plotted as individual points (**0.01; *0.05).

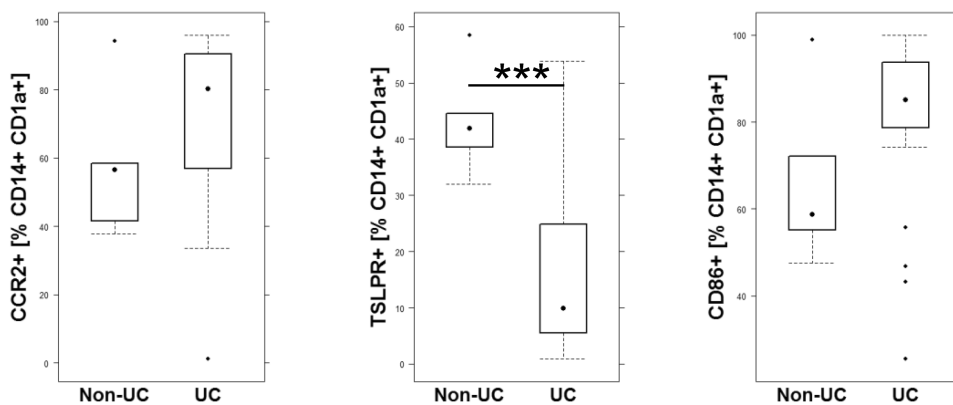


FIGURE 3. Ex vivo analysis of CD14+ CD1a+ monocytes for co-expression of CCR2, CD86, and TSLPR. Flow cytometric analysis of PBMCs from UC patients (n = 21) and non-UC (n = 9) donors depicted as boxplot diagrams. Boxes represent upper and lower quartiles, whiskers represent variability, and outliers are plotted as individual points. For comparison of groups, a Student t test was performed (**0.01; *0.05).

furthermore been identified as natural ligands of CD1a, we wanted to examine whether we could detect a correlation between TAG and CD1a+ CD14+ monocytes in the NSG-UC

mouse model. We first examined whether TAG or cholesterol become elevated in response to challenge. Mice were reconstituted with PBMCs derived from 4 different UC patients.

Following reconstitution with 4×10^6 PBMCs, mice were separated into 2 groups: unchallenged control ($n = 11$) and challenged control ($n = 14$). As shown in Figure 4A, challenge with ethanol results in significantly increased TAG (control: mean \pm SD, 75.36 ± 31.46 ; ethanol: mean \pm SD, 131.0 ± 48.98 ; $P = 0.003$) and cholesterol (control: mean \pm SD, 74.0 ± 31.46 ; ethanol: mean \pm SD, 87.14 ± 13.82 ; $P = 0.003$) levels. In these mice, TAG and cholesterol levels positively correlated with frequencies of CD14+ CD1a+ monocytes (TAG: $\rho = 0.5$, $P = 0.008$, $n = 24$; Cholesterol: $\rho = 0.49$, $P = 0.007$, $n = 25$), indicating that these cells might sense inflammation on a metabolic level to mediate the inflammatory signal to T cells (Fig. 4B).

Anti-CD1a Antibodies Ameliorate Symptoms and Phenotype in NSG-UC Mice

So far, all data indicated a strong proinflammatory response mediated by CD14+ CD1a+ monocytes. In addition, previous studies have shown that CD1a-expressing CD11b+ macrophages

and CD14+ monocytes are highly correlated with the clinical activity score in UC patients and that both cellular populations were found to be elevated in the colon of UC patients.¹⁰ Moreover, both populations had been identified as inflammatory markers in the NSG-UC model (our own results). In order to examine whether inhibition of CD1a affects symptoms and phenotype, anti-CD1a antibodies were tested in the NSG-UC mouse model. Mice were reconstituted with PBMCs derived from 3 different UC patients, 2 of whom were treated with adalimumab and exhibited moderate Simple Clinical Colitis Activity Index (SCCAI) scores of 3 and 5, respectively,¹⁴ and 1 patient was treated with vedolizumab and exhibited a high SCCAI score of 9. In a control experiment, mice were reconstituted with PBMCs derived from a non-UC donor. Following reconstitution with 4×10^6 PBMCs, mice were separated into 3 groups: unchallenged control (non-UC: $n = 4$; UC: $n = 8$), challenged control (non-UC: $n = 4$; UC: $n = 16$), and the study group (non-UC: $n = 4$; UC: $n = 16$), containing challenged mice additionally treated by intraperitoneal injection of anti-CD1a antibodies (30 μ g) on days 7,

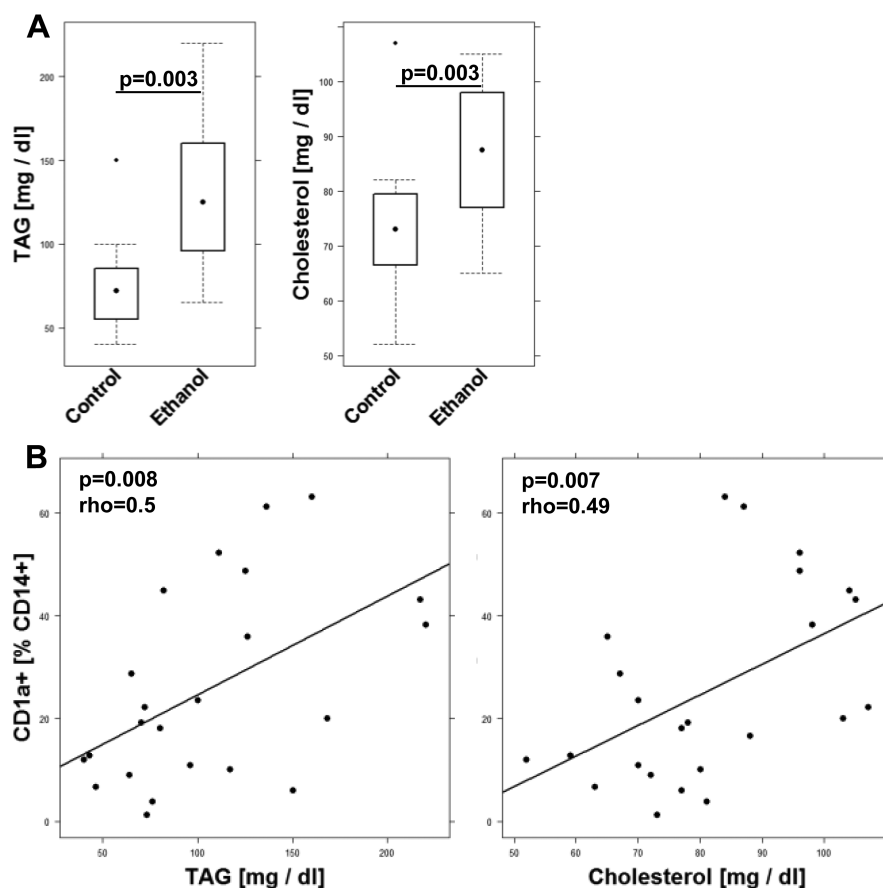


FIGURE 4. TAG and cholesterol levels increase in the NSG-UC mouse model and correlate with CD1a-expressing monocytes. NSG-UC mice were engrafted with PBMCs derived from UC patients ($n = 4$), challenged with 10% ethanol at day 8 and 50% ethanol at days 15 and 18. A, TAG and cholesterol levels depicted as boxplot diagrams; nchallenged group (control, $n = 12$), ethanol challenged group (ethanol, $n = 21$). Whiskers represent variability, and outliers are plotted as individual points. B, Correlation analysis of CD14+ CD1a+ monocytes with TAG and cholesterol levels depicted as scatter plots. (TAG $n = 24$, cholesterol $n = 25$). The method was Spearman; numbers display correlation coefficients (ρ values) and P values.

14, and 17, as described in the Methods section. The challenged control group was treated with 30 µg of isotype control antibodies. Symptoms of colitis were induced by intrarectal challenge of 10% ethanol on day 8, followed by 50% ethanol on days 15 and 18. Mice were monitored throughout the experiment, and symptoms were classified according to a clinical score, as described in the Methods section. As shown in **Figure 5A**, mice developed a clinical activity score upon challenge with ethanol, which was slightly decreased in the study group. As previously described,¹¹ NSG-non-UC mice hardly responded to challenge with ethanol. Anti-CD1a antibodies further diminished the effect of ethanol. Mice were killed on day 21, and the colon was removed and subjected to visual inspection. As shown in **Figure 5B**, the colons of mice in the challenged group revealed lack of pellets, soft pellets, and dilatation, whereas the appearance of the colon of the study group was similar to the unchallenged control group. Colons of the NSG-non-UC mice appeared normal. To further analyze the effect of anti-CD1a antibodies, distal parts of the colon were subjected to histological analysis. As shown in **Figure 5C**, the challenged control groups revealed edema and influx of inflammatory cells, whereas the unchallenged control and treated study group exhibited reduced influx of inflammatory cells and less edema. Some of the mice, however, appeared to have augmented fibrosis (data not shown). This was also reflected in the histological score (**Fig. 5A**).

To analyze the effect of anti-CD1a antibodies on a cellular level, human leucocytes isolated from distal parts or the colon of NSG-UC mice were isolated and subjected to flow cytometric analysis. Due to the low number of cells, samples were pooled from each group. As shown in **Figure 5D**, treatment of mice with anti-CD1a antibodies resulted in a specific decline of CD14⁺ CD1a⁺ monocytes whereas frequencies of TSLPR-expressing CD11b⁺ macrophages and CD14⁺ monocytes increased, suggesting a favoring of the anti-inflammatory response by anti-CD1a antibodies. This hypothesis was also corroborated by RT-PCR analysis performed on distal parts of the colon (for the complete analysis, see **Supplementary Table 4**). As previous studies had identified HGF, IFN γ , TGF β 1, and TARC as markers associated with the acute or remodeling condition of inflammation in NSG-UC mice or UC patients, mRNA expression levels were determined. As shown in **Figure 5E**, levels of mTARC and mTGF β 1 increased in response to treatment, suggesting that inflammation was not completely suppressed but that anti-CD1a antibodies favored a remodeling condition. In contrast, treatment resulted in decreased HGF mRNA, indicating that the acute inflammatory condition was suppressed. Treatment had no effect on IFN γ mRNA levels.

To further examine the effect of anti-CD1a antibodies on the cellular level, human leucocytes were isolated from mouse spleens and subjected to flow cytometric analysis. Previous studies had identified CD14⁺ CD1a⁺ monocytes and CD11b⁺ CD1a⁺ macrophages as cellular markers associated

with inflammation in the NSG-UC model. Thus, the increase of frequencies of both cell types in response to challenge was in agreement with previous results (**Fig. 6A**). Unexpectedly, the same effect was observed in the NSG-non-UC mice. These mice, however, exhibited higher frequencies of TSLPR-expressing monocytes. No difference between healthy and UC donor was observed with respect to monocytes expressing CD64⁺. Treatment of mice with anti-CD1a antibodies resulted in a decrease of CD14⁺ CD1a⁺ monocytes whereas CD11b⁺ CD1a⁺ macrophages remained unaffected. In order to find some evidence on which cellular population CD1a⁺ CD14⁺ monocytes and CD14⁺ macrophages evoked an activity, a correlation analysis was performed (**Fig. 6B**). A positive correlation was observed between CD14⁺ CD1a⁺ and central memory CD8⁺ T cells and unswitched B cells (CD19⁺ CD27⁺ IgD⁺) whereas CD1a⁺ monocytes correlated negatively with switched B cells (CD19⁺ CD27⁺ IgD⁻) and Treg (CD4⁺ CD25⁺ CD127⁻), indicating that CD14⁺ monocytes elicit a CD8 response while suppressing the maturation of B cells. This result is in agreement with previous studies.⁵ In contrast, CD11b⁺ macrophages correlated positively with activated CD4⁺ T cells (CD69⁺), suggesting an entirely different mode of action of these 2 cell types.

DISCUSSION

The role of CD1a in homeostasis or inflammation is far from being understood. The vagueness concerns both the CD1a-expressing macrophages/monocytes and T cells to which these cells convey their signals. In the intestine, where homeostasis, repair, and defense against pathogens relies on the influx of immune cells from the blood into the mucosa, plasticity of immune cells and especially of monocytes might be imperative. Most monocytes develop into macrophages; however, depending on the inflammatory milieu, monocytes can adopt a DC phenotype or develop into fibrocytes and cells with hepatocyte characteristics.^{15,16} And even macrophages have different functions ranging from inflammatory to healing and modulatory. For that reason, macrophages are considered accessory cell types that support their client cells—notably mucosal epithelial cells in the gut—with various functions.¹⁷ Hence, the identification of CD1a on monocytes and macrophages cannot per se be associated with a certain pathological function. In UC patients, CD1a-expressing CD11b⁺ macrophages and CD14⁺ monocytes have been found elevated in the blood and in the colon.¹⁰ While TSLPR-expressing monocytes and macrophage could be associated with the acute condition or the remodeling inflammatory condition, respectively, no such correlation was found for the CD1a-expressing macrophages and monocytes. This was different in the NSG-UC model, where both cell types were correlated with clinical activity score. Macrophages exert their activities in 2 ways: They release cytokines and thus shape the inflammatory milieu, and they convey their signals by inducing T cell activation. Various studies based on *in vitro*

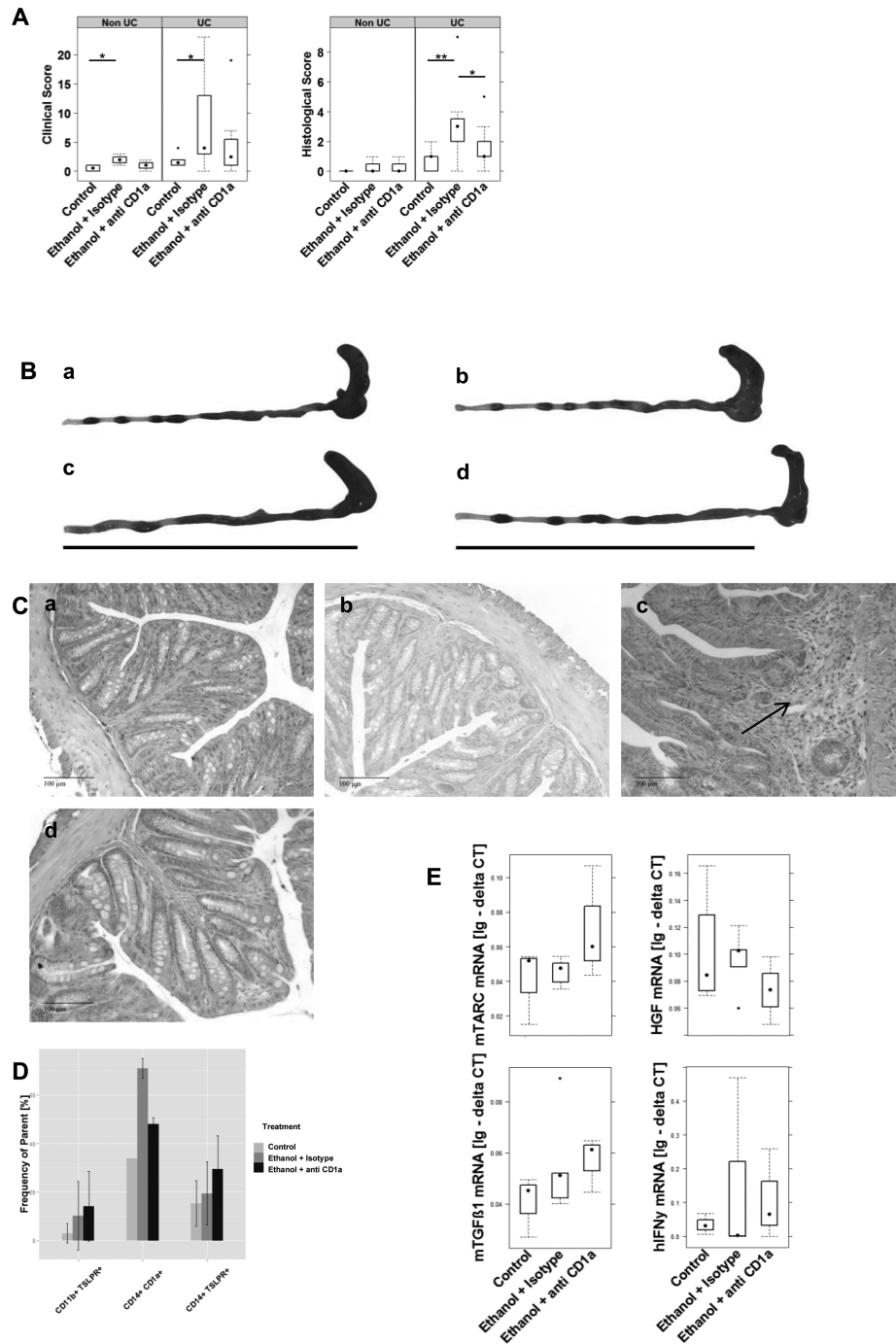


FIGURE 5. NSG-UC mice benefit from treatment with anti-CD1a antibodies. NSG mice were engrafted with PBMCs derived from UC patients (NSG-UC, n = 3) and 1 non-UC donor (NSG-non-UC). Mice were challenged with 10% ethanol at day 8 and 50% ethanol at days 15 and 18 and treated with 30 μg of anti-CD1a antibody or isotype control at days 7, 14, and 17. Control: NSG-non-UC, n = 4; NSG-UC, n = 8. Challenged control (ethanol + isotype): NSG-non-UC, n = 4; NSG-UC, n = 16. Challenged and treated with anti-CD1a antibody (ethanol + anti-CD1a): NSG-non-UC, n = 4; NSG-UC, n = 16. A, Clinical colon and histological scores of NSG-UC mice depicted as boxplot diagrams. B, Macrophotographs of colons at autopsy. a, NSG-UC unchallenged control. b, NSG-non-UC challenged control. c, NSG-UC challenged control, NSG-UC. d, Challenged and treated with anti-CD1a antibody. Arrows indicate edema and influx of inflammatory cells. C, Photomicrographs of H&E-stained sections of distal parts of the colon from mice. Arrows indicate edema and influx of inflammatory cells. D, Frequencies of human leucocytes isolated from colons of mice. Samples from each group were pooled. Mean values are given; error bars are SD. Quantification was performed using flow cytometric analysis. Sample sizes: control n = 3, ethanol + isotype n = 3, ethanol + anti-CD1a n = 3. E, mRNA expression levels of mTARCM, mTGFB1, HGF, and hIFNγ depicted as boxplots. Lg: delta CT, logarithmic delta cycle threshold. Boxes represent upper and lower quartiles. Whiskers represent variability, and outliers are plotted as individual points. Labels given on x-axes on the bottom row apply to all charts. For comparison of groups, ANOVA followed by Tukey's HSD was conducted.

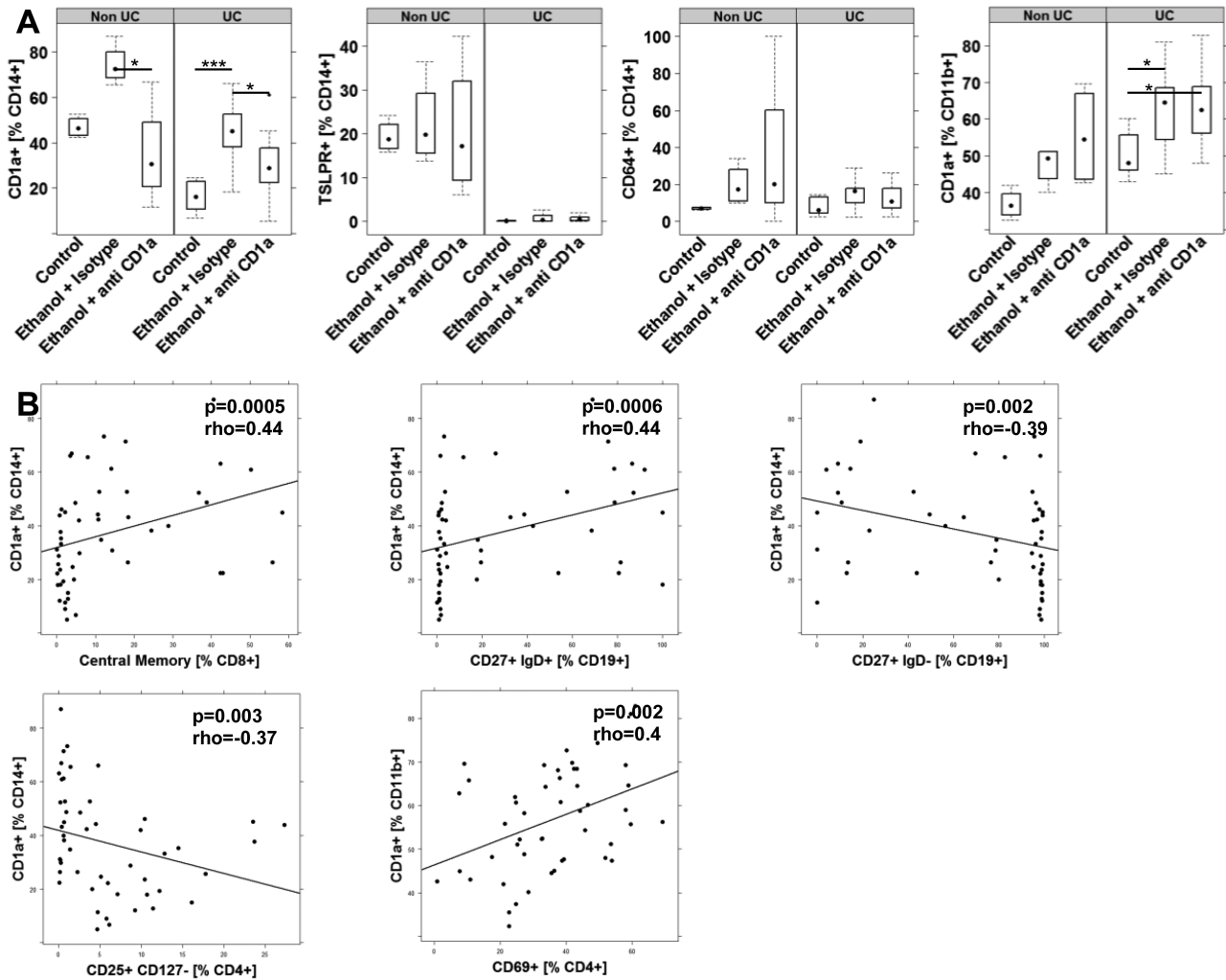


FIGURE 6. Treatment of NSG-UC mice with anti-CD1a antibodies affects CD14+ CD1a+ monocytes. NSG mice were engrafted and treated as in Figure 5. Human leucocytes were isolated from mouse spleen and subjected to flow cytometric analysis. A, Frequencies of CD14+ CD1a+ and CD11b+ CD1a+ cells depicted as boxplot diagrams. Boxes represent upper and lower quartiles. Whiskers represent variability, and outliers are plotted as individual points. B, Correlation analysis of frequencies of CD14+ CD1a+ monocytes with subsets of B and T cells cells depicted as scatter plots. The method was Spearman; numbers display correlation coefficients (*rho* values) and *P* values.

differentiation of DCs from CD34+ hematopoietic stem cells or CD14+ blood monocytes have shown that CD1a expression defines IL-12-producing DCs,^{5, 18, 19} supporting the idea of a proinflammatory phenotype of CD1a-expressing macrophages. In our in vitro study, we have shown that frequencies of CD1a-expressing monocytes were enhanced in the presence of PC, indicating that PC might additionally fuel inflammation by inducing the development of CD1a+ monocytes. The effector function of monocytes and macrophages not only relies on the released cytokines but also on T-cells, which are activated by these cells. It has been shown by in vitro analysis that CD1a expressed on K562 cells to present self-lipids activate Th22 cells to express IL-22, which is thought to play a role in the wound healing processes.⁸ This effect was donor dependent, as only 3 of 6 donors reacted to exposure to CD1a-expressing K562

cells with elevated levels of IL-22. Some of these autoreactive T cells, however, also expressed IFN γ and IL-13, suggesting that the response might not be restricted to Th22 cells. Other in vitro experiments have shown that DC-expressing CD1a directed a Th1 response whereas CD1a- dendritic cells favored a Th2 response.¹⁸ In addition, recent findings suggest that CD1a expressed on Langerhans cells mediate inflammation in poison ivy dermatitis by inducing the release of IL-17 and IL-22 from $\alpha\beta$ CD4+ T cells.²⁰ Furthermore, the fact that memory CD4+ cells isolated from psoriasis patients responded to exposure with autologous CD1a-expressing DCs by increased expression of IL-17 and IL-22 suggests that CD1a-mediated inflammation might also play a role in psoriasis. In the in vitro experiment presented here, CD1a-expressing monocytes induced the activation of CD4+ cells and the frequencies of Th17, Th1, and

Th2 cells. As CD1a is not expressed in mice, in vivo experiments to elucidate the function of CD1a cannot be performed in conventional mouse models. Therefore, the NSG-UC mouse model was used in this study. Mice benefited from the treatment with anti-CD1a antibodies, as indicated by the decreased clinical and histological scores. The beneficial effect was also reflected in the decrease of frequencies of CD1a-expressing CD14⁺ monocytes isolated from the spleen and colon and the decrease of HGF, which had previously been found to be associated as a marker of acute inflammation in UC patients and the NSG-UC mouse model.¹⁰ In contrast, frequencies of TSLPR-expressing monocytes and macrophages and TGF β 1 mRNA expression levels increased in the colon in the presence of anti-CD1a antibodies, suggesting that the suppression of CD1a activity might shift the balance toward a remodeling inflammation, as we have previously observed when patients or mice were treated with infliximab. Thus, CD1a expression on monocytes seemed to provoke a proinflammatory phenotype. The fact that frequencies of CD1a-expressing monocytes similarly increased in NSG-non-UC mice without inducing inflammation suggests that the presence of CD1a-expressing monocytes alone is not sufficient. These mice, however, exhibited much higher levels of TSLPR-expressing monocytes as compared with NSG-UC mice, further supporting the hypothesis that the disturbance of the equilibrium reflected by misbalanced expression of monocyte subtypes might be a driver in UC. The proinflammatory phenotype of CD1a⁺ monocytes was also corroborated by correlation analysis. CD1a⁺ CD14⁺ monocytes correlated positively with central memory CD8⁺ T cells and negatively with Tregs. Both CD1a⁺ and CD1a⁻ macrophages have previously been shown to have the capacity to elicit a cytotoxic T-cell response, although this response was weaker in CD1a⁺ macrophages.¹⁹ Of note, CD1a-expressing monocytes correlated positively with unswitched B cells and negatively with switched B cells, supporting data obtained from in vitro studies that had shown that CD1a DCs mediate T-cell priming whereas CD1a-DCs promote B-cell activation.²¹

This observation, together with the finding that CD14⁺ CD1a⁺ monocytes responded to PC by proliferation or differentiation and correlated positively with TAG levels, suggests that these monocytes not only relay signals but also might sense inflammation and in turn evoke a proinflammatory response. This observation prompted us to further characterize the phenotype of CD1a-expressing monocytes. And indeed, flow cytometric analysis revealed that these populations also expressed TSLPR, CCR2, and the activation marker CD86 to various degrees. Assuming that the expression pattern of non-UC donors reflects the homeostatic situation and that TSLP and, in consequence, TSLPR are essential for maintaining homeostasis in the intestinal mucosa,²² the equilibrium could be maintained by almost equal expression levels of TSLPR and CD1a simultaneously relaying signals toward opposing pathways required by the constant regeneration of the mucosa. In case of

inflammation as in UC, the balance would be shifted toward a proinflammatory phenotype by increased levels of PC or TAG at the expense of a tolerating phenotype mediated by TSLPR. This hypothesis is corroborated by our findings that auto-antibody levels are significantly increased in UC patients (our own results). Metabolic and inflammatory pathways are known to be highly integrated to provide swift energy supply in times of high energy expenditure by immune cells.²³ In addition, the link between monocyte differentiation and lipid metabolism has previously been found and assigned to the activity of PPAR- γ , whose inhibition induces the differentiation of M2 macrophages.²⁴ Furthermore, inducing PPAR- γ activation leads to suppression of TSLP expression, reinforcing the link between TSLP and lipid metabolism.²⁵ The results presented here further elucidate the link by defining CD1a-expressing monocytes as sensors and mediators of inflammation and TSLPR and CD1a as opposing actors in the inflammatory “mobilée.”

SUPPLEMENTARY DATA

Supplementary data is available at *Inflammatory Bowel Diseases* online.

ACKNOWLEDGMENTS

Our special thanks go to the donors; without their commitment, this work could not have been possible. We thank Janina Caesar for excellent technical support and Simone Breitenicher for her excellent support and assistance in recruiting patients. We thank the team in the animal facility for their excellent work and their enduring friendliness in stressful situations.

Ethical considerations: All donors gave informed written consent, and the study was approved by the Institutional Review Board of the Medical Faculty at the University of Munich (2015–22). Animal studies were approved by the ethics committee of the government of Upper Bavaria, Germany (55.2-1-54-2532-65-11 and 55.2-1-54-2532-76-15), and performed in compliance with German Animal Welfare Laws.

REFERENCES

1. Ginhoux F, Williams M. Tissue-resident macrophage ontogeny and homeostasis. *Immunity*. 2016;44:439–49.
2. Gomez Perdiguero E, Klapproth K, Schulz C, et al. Tissue-resident macrophages originate from yolk-sac-derived erythro-myeloid progenitors. *Nature*. 2015;518:547–51.
3. Bain CC, Bravo-Blas A, Scott CL, et al. Constant replenishment from circulating monocytes maintains the macrophage pool in the intestine of adult mice. *Nat Immunol*. 2014;15:929–37.
4. Suzuki A, Masuda A, Nagata H, et al. Mature dendritic cells make clusters with T cells in the invasive margin of colorectal carcinoma. *J Pathol*. 2002;196:37–43.
5. Cernadas M, Lu J, Watts G, et al. CD1a expression defines an interleukin-12 producing population of human dendritic cells. *Clin Exp Immunol*. 2009;155:523–33.
6. Van Rhijn I, van Berlo T, Hilmenyuk T, et al. Human autoreactive T cells recognize CD1b and phospholipids. *Proc Natl Acad Sci U S A*. 2016;113:380–5.
7. de Jong A, Cheng TY, Huang S, et al. CD1a-autoreactive T cells recognize natural skin oils that function as headless antigens. *Nat Immunol*. 2014;15:177–85.
8. de Jong A, Peña-Cruz V, Cheng TY, et al. CD1a-autoreactive T cells are a normal component of the human $\alpha\beta$ T cell repertoire. *Nat Immunol*. 2010;11:1102–9.

9. Birkinshaw RW, Pellicci DG, Cheng TY, et al. A β T cell antigen receptor recognition of CD1a presenting self lipid ligands. *Nat Immunol.* 2015;16:258–66.
10. Föhlinger M, Palamides P, Mansmann U, et al. Immunological profiling of patients with ulcerative colitis leads to identification of two inflammatory conditions and CD1A as a disease marker. *J Transl Med.* 2016;14:310.
11. Palamides P, Jodeleit H, Föhlinger M, et al. A mouse model for ulcerative colitis based on NOD-scid IL2R γ null mice reconstituted with peripheral blood mononuclear cells from affected individuals. *Dis Model Mech.* 2016;9:985–97.
12. Bourgeois EA, Subramaniam S, Cheng TY, et al. Bee venom processes human skin lipids for presentation by CD1a. *J Exp Med.* 2015;212:149–63.
13. Feingold KR, Grunfeld C. The effect of inflammation and infection on lipids and lipoproteins. In: De Groot LJ, Chrousos G, Dungan K, et al., eds. *Endotext.* South Dartmouth, MA: 2000.
14. Walmsley RS, Ayres RC, Pounder RE, Allan RN. A simple clinical colitis activity index. *Gut.* 1998;43:29–32.
15. Benesic A, Rahm NL, Ernst S, et al. Human monocyte-derived cells with individual hepatocyte characteristics: a novel tool for personalized in vitro studies. *Lab Invest.* 2012;92:926–36.
16. Oh MH, Oh SY, Yu J, et al. IL-13 induces skin fibrosis in atopic dermatitis by thymic stromal lymphopoietin. *J Immunol.* 2011;186:7232–42.
17. Okabe Y, Medzhitov R. Tissue biology perspective on macrophages. *Nat Immunol.* 2016;17:9–17.
18. Chang CC, Wright A, Punnonen J. Monocyte-derived CD1a+ and CD1a- dendritic cell subsets differ in their cytokine production profiles, susceptibilities to transfection, and capacities to direct th cell differentiation. *J Immunol.* 2000;165:3584–91.
19. Ratzinger G, Baggers J, de Cos MA, et al. Mature human langerhans cells derived from CD34+ hematopoietic progenitors stimulate greater cytolytic T lymphocyte activity in the absence of bioactive IL-12p70, by either single peptide presentation or cross-priming, than do dermal-interstitial or monocyte-derived dendritic cells. *J Immunol.* 2004;173:2780–91.
20. Kim JH, Hu Y, Yongqing T, et al. CD1A on langerhans cells controls inflammatory skin disease. *Nat Immunol.* 2016;17:1159–66.
21. Liu YJ. Dendritic cell subsets and lineages, and their functions in innate and adaptive immunity. *Cell.* 2001;106:259–62.
22. Park JH, Jeong DY, Peyrin-Biroulet L, et al. Insight into the role of TSLP in inflammatory bowel diseases. *Autoimmun Rev.* 2017;16:55–63.
23. O'Neill LA, Kishton RJ, Rathmell J. A guide to immunometabolism for immunologists. *Nat Rev Immunol.* 2016;16:553–65.
24. Zizzo G, Cohen PL. The PPAR- γ antagonist GW9662 elicits differentiation of M2c-like cells and upregulation of the MerTK/Gas6 axis: a key role for PPAR- γ in human macrophage polarization. *J Inflamm (Lond).* 2015; 12:36.
25. Sziksz E, Molnár K, Lippai R, et al. Peroxisome proliferator-activated receptor- γ and thymic stromal lymphopoietin are involved in the pathophysiology of childhood coeliac disease. *Virchows Arch.* 2014;465:385–93.